UNIVERSIDADE DA BEIRA INTERIOR
Engenharia

Manufacture and characterization of epoxy composites doped with Fe_3O_4 and SiO_2 particles

(versão corrigida após defesa)

Jose Francisco Molina García

Dissertação para obtenção do Grau de Mestre em

Engenharia Aeronáutica

(ciclo de estudos integrado)

Orientador: Prof. Doutor Abílio Manuel Pereira da Silva

Covilhã, Julho de 2019

To the moon and back -A-

Aknowledgments

To the University of Beira Interior, in particular to the Department of Aerospace Sciences and to the Department of Electromechanical Engineering, for having made available the facilities, equipment and materials.

To the Center of Mechanical and Aerospace Science and Technologies (C-MAST-UBI), C-MAST-UID/EMS/00151/2019, for the availability of laboratory resources and support to external services.

To Prof. Abílio Silva, for the supervision and guidance and his help and full availability to make possible to complete this work.

To Prof. Paulo Reis, Dr. Marco Silva and MSc. Paulo Santos for the availability and support in the manufacture and in the experimental tasks of characterization of the mechanical behavior.

To Doctor Alberto Maceiras for the support in physical, DSC and fracture toughness tests.

At the Optics Center, namely Dr. Ana Paula Gomes for the DSC tests and micrograph images and Mr. Óscar Rato for the help in the preparation of the samples.

This Master Dissertation has been supported by the project Centro-01-0145-FEDER-000017 - EMaDeS - Energy, Materials and Sustainable Development, co-financed by the Portugal 2020 Program (PT 2020), within the Regional Operational Program of the Center (CENTRO 2020) and the European Union through the European Regional Development Fund (ERDF).

Cofinanciado por:

UNIÃO EUROPEIA
Fundo Europeu
de Desenvolvimento Regional

Resumo

Polímeros termoendurecíveis são amplamente utilizados na indústria aeroespacial. Um dos polímeros termoendurecíveis mais comuns é a resina epóxi, que é amplamente utilizada como matriz de compósitos reforçados com fibras, em particular fibras vidro e fibras de carbono. As propriedades destes polímeros de base epoxídica podem ser melhoradas com a adição de outros materiais particulados ou de pequenas fibras tendo em vista a construção de uma resposta mecânica estruturada de forma hierárquica (nano – micro- macro).

Com este trabalho pretende-se estudar o efeito da adição de partículas de óxidos numa resina epóxi. Isto é fabricar e caracterizar a influência da adição de óxido de ferro (magnetite, Fe_3O_4) e sílica de fumo (SiO_2), em diferentes quantidades: 0,25 wt%, 0,5 wt% e 1 wt%, e 2 wt% e 4 wt% de Fe_3O_4 e SiO_2, respetivamente. Para isso, realizaram-se ensaios de resistência mecânica em flexão de três pontos, relaxamento de tensões e de tenacidade à fratura; Ensaios físicos de porosidade aparente e de densidade aparente e ensaios de calorimetria. Os resultados são analisados e discutidos em função da evolução das propriedades tendo em consideração a quantidade de aditivos e com a literatura.

Os resultados obtidos mostram que a adição de partículas de SiO_2 fumed leva a uma melhora em σ_{max}, módulo de Young, K_{IC} e relaxamento de tensões; enquanto a adição de partículas de Fe_3O_4 diminui o valor de sem melhora significativa no restante das propriedades estudadas. Além disso, a adição de ambos os enchimentos leva a uma diminuição da T_g.

Palavras-chave

Resina epóxi, Fe_3O_4, SiO_2, Mistura com ultrassons, Flexão em 3 pontos, Relaxamento de tensões, Tenacidade à fratura, Porosidade

Abstract

Thermosetting polymers are widely used in the aerospace industry. One of the most commonly used thermoset is the epoxy resin, which is widely used as the matrix phase of carbon and glass fibre reinforced composite. The properties of these epoxy-based polymers can be improved with the addition of other particulate or small fibre materials in order to construct a hierarchically structured (nano-micro-macro) mechanical response.

This work intends to study the effect of the addition of oxide particles on an epoxy resin. This is to manufacture and characterize the influence of the addition of iron oxide (magnetite, Fe_3O_4) and silica fumed (SiO_2) in different amounts: 0.25 wt%, 0.5 wt% and 1 wt%, and 2 wt% and 4 wt% Fe_3O_4 and SiO_2, respectively. For this, mechanical resistance in three-point bending, tensile relaxation and fracture toughness were performed; also physical tests of apparent porosity, apparent density and calorimetry tests were conducted. The results are analyzed and discussed according to the evolution of the properties taking into account the quantity of additives and the literature.

The obtained results show that the addition of SiO_2 fumed particles leads to an improvement in σ_{max}, Young's modulus, K_{IC} and stress relaxation whereas the addition of Fe_3O_4 particles decreases the value of σ_{max} with no significant improvement in the rest of studied properties. Moreover, the addition of both fillers leads to a decrease of T_g.

Keywords

Epoxy resin, Fe_3O_4, SiO_2, Ultrasonic mixing, Flexural properties, Stress relaxation, Fracture toughness, Porosity.

Table of contents

List of figures

Chapter 4.

List of tables

Chapter 2.

Chapter 3.

Chapter 4.

Acronyms

Al_2O_3	Alumina
ASTM	American Society for Testing Materials
BMI	Bismaleimide
BNNP	Boron Nitride Nanoparticles
BNNS	Boron Nitride Nanosheets
BNNT	Boron Nitride Nanotubes
$CaCO_3$	Calcium carbonate
CFRP	Carbon Fiber Reinforced Composite
CMC	Ceramic Matrix Composite
CNT	Carbon Nanotubes
DSC	Differential Scanning Calorimetry
EMI	Electromagnetic Interference
EDX	Energy-dispersive X-ray
Fe_2O_3	Ferric oxide (hematite)
Fe_3O_4	Iron oxide (magnetite)
GNP	Graphene Nanoplatelets
MA	Microwave Absorption
MMC	Metal Matrix Composite
NP	Nanoparticles
OAT	Oxyamino Triazine
PEEK	Polyether Ether Ketone
PEI	Polyetherimide
PMC	Polymer Matrix Composite
PMMA	Polymethyl Methacrylate
PPS	Polyphenylene Sulfide
SENB	Single Edge Notch Bend
SiO_2	Silica

TiO_2 Titanium dioxide

Symbols

P_A	Aparent porosity
R	Crosshead motion rate
T_c	Crystallization temperature
D	Deflection at the center of the beam
ρ	Density
ρ_m	Density of the matrix
ρ_f	Density of the reinforcement
D_w	Dry weight
V_e	Exterior volume
G_{IC}	Fracture energy
K_{IC}	Fracture toughness
T_g	Glass transition temperature
P_b	Load at the break
P	Load of the force applied
m	Mass
σ_{max}	Maximum stress
T_m	Melting temperature
ρ_r	Relative density
W	Saturated weight
d	Specimen thickness
b	Specimen width
ε	Strain
ε_{max}	Strain at maximum stress
σ	Stress
L	Support span
S	Suspended weight
ρ_{th}	Theoretical density

P_T Total porosity

V Volume

V_m Volume fraction of the matrix

V_f Volume fraction of the reinforcement

W_m Weight fraction of the matrix

W_f Weight fraction of the reinforcement

Chapter 1. Introduction

In this chapter the project is framed inside the aeronautical sector, remarking the importance of polymers in this industry specially as a matrix phase of a composite material. The objectives are also established and the structure of this document is also presented and explained.

1.1. Project framing

The evolution of the human being is strongly linked with the evolution of the materials. A prove of this statement resides in the fact that the first stages of prehistory are determined by the use of different materials [1]. The same thing happens when talking about the aeronautical industry. In this sector, the changes in the main criteria for selection of the materials have pushed the research of new materials. From the very beginning, when the objective was to obtain the maximum strength with the minimum weight, to a modern goal such as the reduction of greenhouse gas emissions [2]. A summary of these new criteria's introduction can be seen in Figure 1.1. For that, the main materials have suffered a drastically change in all those years, starting with aircrafts whose predominant material were wood.

As commercial aviation became more popular, and the military one realized about the advantages that fast fighters meant, there was an important change in the aircraft design. High stiffness or durability were now an important issue at the time of selecting materials for flying faster and longer. These new criteria's lead not only to new materials but to new production methods in order to obtain aircraft components from these materials. At that time, aluminum alloys were started to be used in aircrafts, which would be the most dominant materials for a long time. Other materials were started to be implemented in the following years in order to improve fracture toughness, fatigue resistance or even heat-resistance when supersonic flights appeared such as titanium alloys, superalloys and CMCs.

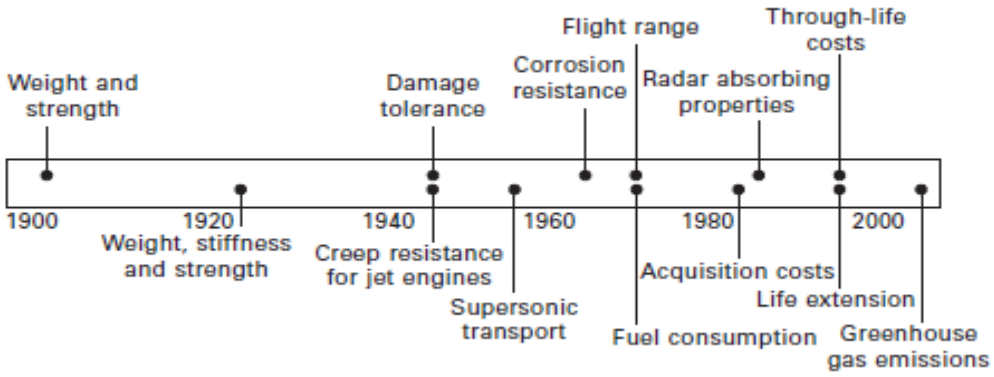

Figure 1. 1. Historical timeline of the introduction of key criteria in aeronautics (Adapted from [3])

It was not until the fuel crisis in the 1970s when the next big materials were introduced. These were the carbon-epoxy composites which were first introduced in secondary structures. However, the first composite materials used in the aeronautical sector were glass fibers in a low-strength polymer matrix in the 1940s. Although their first use was small due to the high cost of carbon fibers and the understanding of its manufacture, as these manufacturing processes improved and the costs of the fibers decreased, the applications of composite materials increased during the 1980s and 1990s.

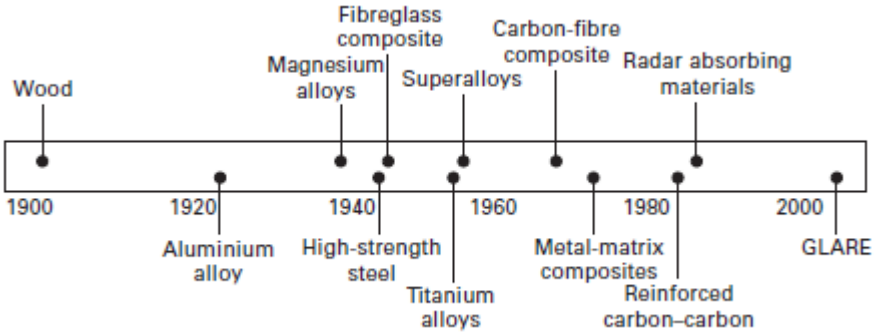

Figure 1. 2. Historical timeline of the first used of some materials in aircrafts (Adapted from [3])

Nowadays, composite materials fight with the long-held dominant position of aluminum. They are used in the fuselage and wings of modern aircrafts such as the Airbus 380 and Boeing 787, with around a 50% of its weight being carbon fiber reinforced composites [4]. Moreover, their use has increased drastically in helicopter components like the body and rotor blades in the recent years [3].

But not only polymer matrix composites (PMCs) are used in the aeronautical sector, others such as metal matrix composites (MMCs) and ceramic matrix composites (CMCs) have

some applications. Especially, CMCs are largely used in break discs for aircrafts or heat shield on space shuttles.

The use of polymers is mainly argued by their low density, which means a low weight. Moreover, they are cheap and its manufacturing process is not complex. However, they present some disadvantages such as low electrical conductivity, low stiffness, poor magnetic properties, low resistance at high temperatures and, in some cases, mechanical properties that are not good enough for some applications. For that reason, some materials can be added to these polymers as fillers, in order to improve some properties that can lead to new applications [5].

1.2. Objectives definition

The aim of this dissertation is to study the use of polymers and composites (polymeric resin doped) with potential use in the aeronautical sector. Moreover, the use of fillers is studied too by means of a bibliographic review and the experimental study.

Manufacture process of the addition, mixing of different fillers and cured; the effect in several properties, such as flexural properties, stress relaxation and toughness properties, apparent density and porosity, and even glass transition temperature is analyzed.

1.3. Document structure

This dissertation is divided in 5 chapters.

In Chapter 1 the topic of this project is framed inside the aeronautical sector, focusing on the importance of polymers in it. Moreover, the objectives of the work are established and the structure of this document is described.

In Chapter 2 the use of polymers in the aeronautical sector is explained in a more detailed way, along with the use of fillers. For doing that, some previous scientific articles are analyzed.

In Chapter 3 the materials that have been used in this project are presented as well as the manufacturing process that has been followed and the applied mechanisms in order to characterize the obtained materials.

In Chapter 4 the results of the tests that have taken place are presented and analyzed in order to be able to study them.

In Chapter 5 the previous results are discussed and the obtained conclusions are summarized. The further work is proposed.

Chapter 2. State of Art

In this chapter, a short theoretical review of what a polymer and a composite material are is done. There is also a recapitulation of the evolution of the use of polymers and composites in the aeronautical sector along with an explanation of the different applications of them. Furthermore, there is a review of the literature about the use of fillers in order to enhance the properties of a resin.

2.1. Polymers in aeronautical industry

A polymer is a macromolecule formed by monomers, smaller structural units which are molecules with a small molecular mass that, after the polymerization reactions, form the polymeric macromolecules. There are two main types of polymerization: by condensation or by addition. Polymers can be divided in three main groups: thermoplastics, thermosets and elastomers. In the aeronautical sector, polymers are usually applied as the matrix phase in fiber reinforced composites but they are also used as an adhesive for joining structural components [5].

This kind of materials have several useful properties for an aircraft material. These properties depend on the type of polymer but some of them are common for the three of them: low density, moderate cost and good corrosion resistance. However, they present some disadvantages that do not allow them to be used on their own such as low stiffness, strength or working temperature. Table 2.1 sums up the main advantages and disadvantages of the three groups of polymers.

The most widely used kind of polymers in aeronautics are the thermosetting ones. Inside this group, it can be highlighted the epoxy resin. These are the most used in aircraft structures based on their low shrinkage, high strength and good durability in hot and moist environments. Despite that, they cannot be safely used inside cabins due to poor fire performance, what means that they ignite in an easy way and release lots of heat and smoke. That is why phenolic resins are used on most of the internal components [5]. Apart from these two examples, other thermosets deserved to be mentioned, such as bismaleimides (BMIs). Phenolic-triazine resins or polybenzoxazine [6]. Some properties of these thermosetting polymers are summed up in the Table 2.2. As it can be seen in this table, epoxy resin do not outstand for any of their properties but it is the combination of all of them that makes them an “all-rounder” [6].

Table 2. 1. Advantages and disadvantages of the three main kind of polymers (Adapted from [5])

Thermoplastic	Thermoset	Elastomer
Advantages		
• No cure required • Rapid processing • High ductility • High fracture toughness • High impact resistance • Can be recycled	• Low processing temperature • Low viscosity • Good compression properties • Good fatigue resistance • Good creep resistance • Highly resistant to solvents • Good fiber wetting for composites	• Low processing temperature • High ductility and flexibility • High fracture toughness • High impact resistance
Disadvantages		
• Very high viscosity • High processing temperature • Poor creep resistance	• Long processing time • Low ductility • Low fracture toughness • Low impact resistance • Limited shelf life • Cannot be recycled	• Long processing time • Poor creep resistance • Low Young's modulus • Low tensile strength

Table 2. 2. Properties of main thermosets (Adapted from [6])

	High Performance Epoxy	Phenolic	Toughened BMI	Phenolic-triazine	Polybenzoxacine
Tensile strength (MPa)	90-120	24-25	50-90	4.2	100-125
Tensile modulus (GPa)	3.1-3.8	3-5	3.5-4.5	4.1	3.8-4.5
T_g (ºC)	150-220	170	230-280	300-400	170-340
Max. temperature of use (ºC)	180	200	200	300	130-280
Density (g/cm^3)	1.2-1.25	1.24-1.32	1.2-1.3	1.25	1.197
K_{IC} ($MPa \cdot m^{1/2}$)	0.6	1.01	0.85	0.2-0.3	0.6-1.1

Even though they are much less used than thermosets, thermoplastics are also applied to the aeronautical industry as the matrix phase of a composite material or as a structural adhesive, and their use is gradually increasing. In fact, they present some advantages when using them in a composite, such as better impact damage resistance, higher fracture toughness. However, thermoplastics have to be processed at higher temperature which causes that they

were more expensive to manufacture [5]. Some of the most common thermoplastics are polyether ether ketone (PEEK), polyphenylene sulfide (PPS), polyetherimide (PEI) or polycarbonate, which properties are summed up in Table 2.3.

Table 2. 3. Properties of main thermoplastics (Adapted from [5])

	PEEK	PPS	PEI	Polycarbonate
Flexural strength (MPa)	170	100-120	100-177	103.4
Tensile strength (MPa)	89.6	65-85	91.9-101.4	65.5
Young modulus (GPa)	3.66	3.3-4	2.89-3.04	2.6
T_g (ºC)	146	85	217	145
Thermal conductivity (W/mK)	0.2	0.3	0.06	0.19-0.22
Density (g/cm^3)	1.32	1.35	1.27	1.2

Moreover, some thermoplastics are used because they are transparent, tough and impact resistant to manufacture windows and canopies, such as acrylic plastics and polycarbonates. One of the most common acrylic plastics is the polymethyl methacrylate (PMMA), which is commercialized as *Plexiglass* or *Perspex*. PMMA are lighter, stronger and tougher than common window glass. Furthermore, polycarbonates are even stronger and tougher than acrylic plastics, that is why they are commonly used to manufacture cockpit windows, because they provide good safety [5].

2.2. Adhesive bonding

Another area where polymers are of great interest are adhesives, in particular structural adhesives. An adhesive bonding is a joining process in which an adhesive is placed between two materials and after it solidifies it produces an adhesive bound [7]. These adhesive bonding provides a great alternative to mechanical fastener that are conventionally used such as rivets and screws.

Adhesive bonding presents lower structural weight and fabrication cost and better damage tolerance than common fasteners. Furthermore, they offer more flexibility at the time of designing. They are very useful when applied to fiber reinforced composites due to avoid of discontinuities caused by fastener methods. As the bound is homogeneous and continuous

throughout the surfaces, there are not stress concentrations, so the structural integrity is improved [7].

The first structural application of adhesive bonding dates from 1941. Back then, De Bruyne and Newall developed a phenol-formaldehyde based adhesive commercially known as Redux. It was used in aircrafts such as the British Comet and the Nimrod [8].

Along all these years, adhesives have been developed in order to be able to replace the fastener methods. Nowadays, the adhesives used in structural applications are more and they have different characteristics, which enlarges the scope of possible applications for them. Table 2.4 shows a summary of the different adhesives in the market and their characteristics, given by M. D. Banea and L. F. M da Silva [7].

Table 2. 4. Characteristics of different adhesives in the market (Adapted from [7])

Epoxy	• High strength and temperature resistance • Relatively low cure temperatures • Easy to use • Low cost
Cyanoacrylates	• Fast bonding capability to plastic and rubber • Poor resistance to moisture and high temperatures
Anaerobics	• Can fasten and seal when a tight seal must be formed without light, heat or oxygen • Suitable for cylindrical shapes
Acrylics	• Fast curing • Tolerate dirtier and less prepared surfaces
Polyurethanes	• Resistance to fatigue • Good impact resistance • Durability • Good flexibility at low temperatures
Silicones	• Excellent sealant for low stress applications • High degree of flexibility • Very high temperature resistance • Can seal or bond materials of various natures • Long cure times • Low strength
Phenolics	• Good strength retention for short periods of time • Limited resistance to thermal shocks
Polyimides	• Good thermal stability • Difficult processability

Many factors influence the quality of the bonding. For instance, humidity, UV radiation, solvent exposition or big temperature amplitudes can influence the durability of the bonding if the adhesive is wrongly chosen, threated or isolated [9]. Another important matter is the curing method which must be strictly followed as the manufacturer describes. Moreover, the manufacturing environment should be clean to avoid contamination.

The adherent surfaces are cleaned and pretreated. This is probably the most important factor to determine the quality of the bonding [10]. The surface preparation improves the bond strength and its durability by increasing surface tension, surface roughness and changing the surface chemistry.

2.3. Composite materials

Composites are a group of materials that are made from the mixture of, at least, two different chemical materials with different interface between them [11], that gives a combination of better properties from the properties on their own [12]. A composite consists of a matrix and a reinforcement phase. Usually, the material of the matrix phase has a higher ductility, whereas the reinforcement material is stiffer and stronger [3].

Composite materials can be classified in three main groups according to the material that the matrix is made of: metal matrix composites (MMC), ceramic matrix composites (CMC) and polymer matrix composites (PMC). In the aeronautical sector, the most applied group is the PMCs being the polymer used for the matrix a thermosetting resin like epoxy or, occasionally, a high-performance thermoplastic such as polyether ether ketone (PEEK), while MMCs and CMCs are applied in much less components [3].

There is also a different classification for composites depending on the shape of the reinforcement: particle-reinforced, whisker-reinforcement and fiber-reinforcement.

Since the 1990s, the use of composites, especially fiber-reinforced composites, has increased in the aeronautical industry, being nowadays competing with aluminum alloys to be the dominant material. The reasons for that are the reduction of weight, the increase of strength and stiffness and the reduction of corrosion issues. Figure 2.1 shows the evolution of the content of composite in military and civil aircrafts along the years.

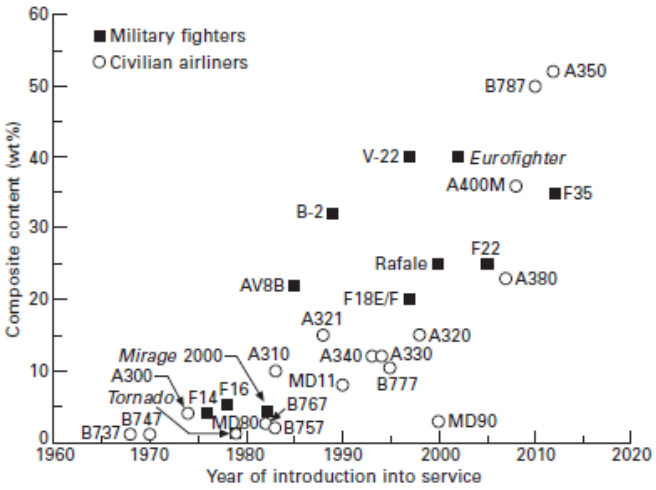

Figure 2. 1. Evolution of composite content along the years (Adapted from [3])

The use of composites presents some general advantages but, on the other hand, they also have some points against them.

Advantages:

- Reduction of weight
- Improvement of the structural efficiency
- Better fatigue and corrosion resistance
- Low thermal expansion coefficient

Disadvantages:

- Higher cost that aluminium
- Slow manufacturing
- Anisotropic properties
- Low impact damage resistance
- Flammability
- Lower temperature operating limit
- Low electrical conductivity

The applications of composites have been led by the military sector, where carbon-fiber reinforced composites (CFRC) are used in primary structures such as the fuselage or the wings, in order to reduce weight and achieve a high structure efficiency. Figure 2.2 shows the use of composites in a fighter, specifically in the F-35. Furthermore, their radar absorption properties and their heat insulation provide military aircrafts with a great advantage, making them more difficult to detect by using radars or infrared devices [4].

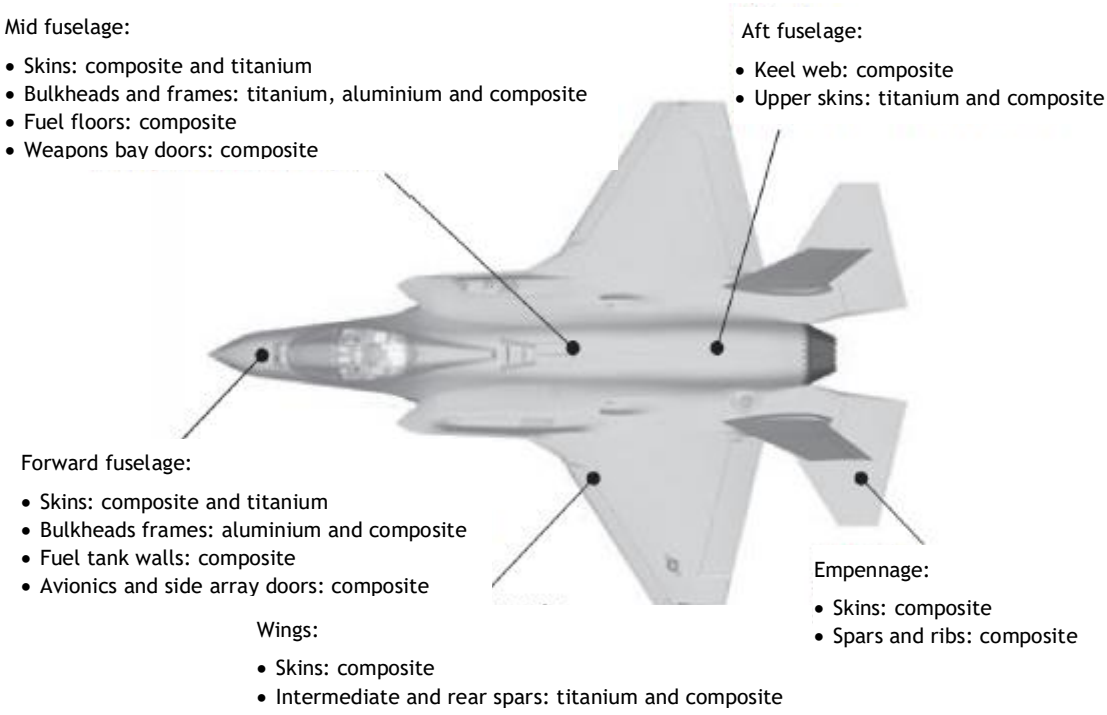

Figure 2. 2. Use of composites in the F-35 (Adapted from [4])

In civil aircrafts, the first primary structure where a composite material was used was the horizontal stabilizer of the Boing 737, certified in 1982. Its use was developed in the 1990s. In Figure 2.3 the typical applications are shown.

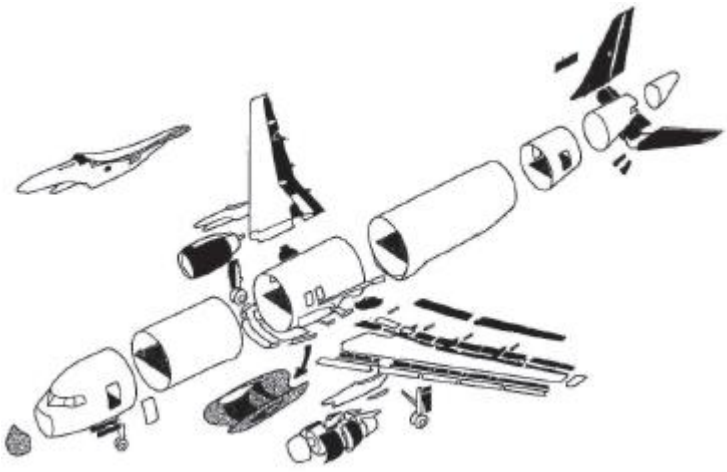

Figure 2. 3. Typical applications of composites (shaded in black) in an aircraft (Adapted from [4])

With the Airbus 380 a huge milestone was reached. This aircraft with 280 tons of weight were made with a 25% of composite materials [4]. Figure 2.4 shows the application of composites, especially CFRCs, in this aircraft.

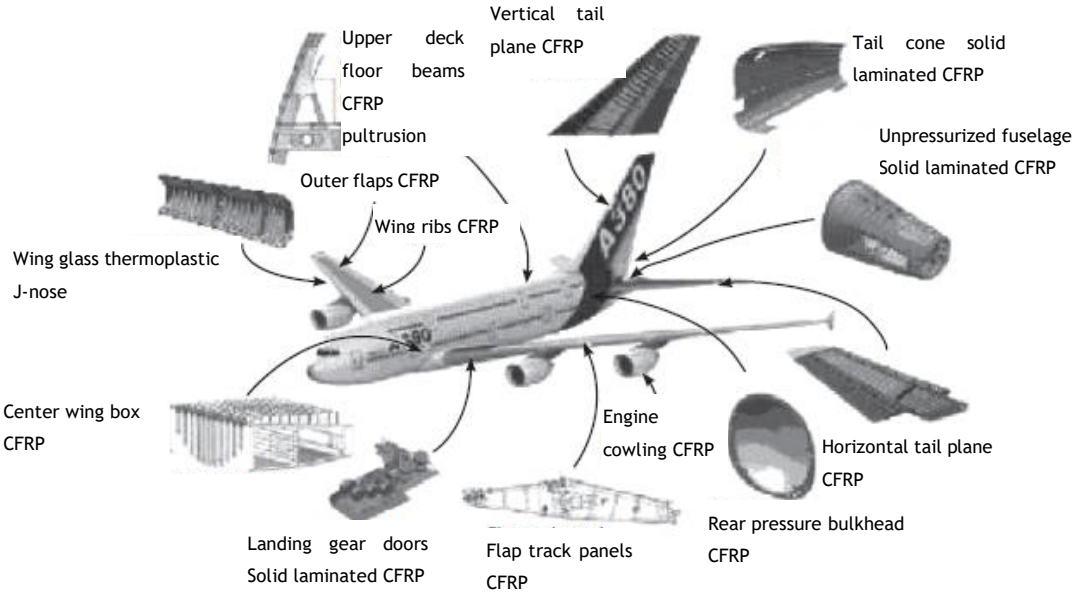

Figure 2. 4. Components made of CFRP of the A380 (Adapted from [4])

The latest in use of composites is the Boeing 787 with a 50% of its weight in CFRC. Also the Airbus 350 with almost a 50% of its structural mass being composite materials. Table 2.5 presents the different applications of composite materials that Boeing and Airbus present in their airliners.

In the case of helicopters, composites are used in the fuselage and rotor blades. Also composites reinforced with fibers of carbon, glass or aramid are applied in the main body and the rotor boom of some helicopters to reduce weight, vibrations and corrosion and improve the structural efficiency [4].

Apart from the aircrafts themselves, composites are also used in some gas turbine engines. For instance, they appear in fan blades, front fan case or bypass ducts. The use of composite materials is restricted for temperatures lower than 150ºC. This is due to possible softening and heat distortion [4]. The reasons for employing composites in these engines are the reduction of weight, the improvement of the structural performance and the decrease of the operational and maintenance costs. In this case, the reduction of weight has a big impact because light fan blades mean that the weight of other components will be reduced too, with its consequent fuel saving and, consequently, increment of the range of operation. Furthermore, this reduction of the weight of the blades reduce the centrifugal force, improving the fatigue life.

Table 2. 5. Composite components in Airbus and Boeing airliners (Adapted from [4])

Composite component	Airbus	Boeing
Fuselage	A380	B787
Belly fairing	A380	
Rear pressure bulkhead	A340-600 A380	
Floor beams	A350 A400M	B787
Keel beam	A340-600 A380	
Nose cone	A340-600 A380	B787
Wingbox	A380 A400M	B787
Wing beams	A350 A380	B787
Wing skins	A350 A380	B787
Horizontal stabilizer	A340 A350	B737 B777 B787
Vertical tailplane	A380	B777
Nacelles	A340 A380	B787
Reversers	A340 A380 A350	
Fan blades		B787
Cone spinners		B787

2.4. Failure in composite structures

The correctly selection of the fiber orientation in a fiber reinforced composite is fundamental to avoid delamination or separation between layers. This delamination occurs due to the developement of interlaminar stresses due to a mismatch in the Poisson's ratio or shear extension coupling between adjacent layers.

Laminated stractures can present two different types of damage: process induced damage and service induced damage [11]. Process induced damages are defects caused by problems during fabrication such as porosity, fiber waviness, delamination, debonding or surface scratches. Furthermore, service induced damages are originated by the mechanical and chemical conditions during service period. Some examples are abrasion, oxidation and swelling due to aggresive environments or matrix cracking, fiber breakage, penetration or hole enlongation due to mechanical overloads [12].

When talking about adhesive bonds, thera are also possible failures. According to the standard ASTM D5573 for standard practice for classifying failure modes in fiber-reinforced plastic joints [13], there seven characterized modes of failure in adhesive joints of fiber reinforced polymers.

2.5. Use of fillers

Epoxy resins are widely used in aeronautics as adhesives or as the matrix phase of a composite material. But in order to improve some of their properties and enlarge the scope of applications, these resins are usually reinforced with fillers. Usually, the addition of fillers looks for improving mechanical and thermal properties. However, they can improve other properties such as electrical or magnetic properties, or even a combination of them (multifunctional components). For that reason, there are a great number of researches about the impact that the addition of different materials can have in the properties of the resin.

Some examples of the addition of fillers that improved the mechanical properties of an epoxy resin are presented after this.

D. Bazrgari et al. [14] stated that with the addition of Al_2O_3 nanoparticles (NPs) into an epoxy resin flexural strength (15%), stiffness and impact strength improved for 1 vol% of Al_2O_3 and the wear rate and friction coefficient decreased for the same amount of filler. Furthermore, V. Eskizeybek et al. [15] studied the effect of the addition of $CaCO_3$ NPs in the epoxy resin itself but also in a CFRC. This study showed improvements for a 2 wt% of $CaCO_3$ in tensile strength (22.2% for the epoxy and 48.4% for the CFRC), statically toughness (37% for the epoxy and 78.6% for the CFRC), flexural load (53.4% for the epoxy and 46.8% for the CFRC) and

deflection (56.5% for the epoxy and 76.2% for the CFRC). Furthermore, there was an improvement of the critical threshold forces of the CFRC of 16.8%, 13.4% and 11.3% for 2m/s, 2.5m/s and 3m/s respectively.

S.K. Singh et al. [16] added TiO_2 microparticles and NPs into the epoxy resin and observed an improve in the tensile strength and ductility, being this improvement higher for a 4 wt% of NPs (43.70% in tensile strength). It also showed an increase of 141.85% in the fracture toughness (K_{IC}) and the fracture energy (G_{IC}) improved too, while the study of the addition of Fe_2O_3 NPs carried out by T. Sun et al. [17] showed that an epoxy resin filled with a 4 wt% of Fe_2O_3 the tensile strength improved in a 50.2% while fracture toughness (K_{IC}) improved in a 106%.

Rajadurai A. et al. [18] tried also the addition of Fe_2O_3 particles obtaining improvements on the tensile, flexural and impact strength and the thermal conditions of a 55.4%, 9.7%, 23.9% and 36% respectively. Moreover, N. Saleh et al. [19] observed the behavior of an epoxy resin with the addition of fly ash and silica fumed. The results showed that the addition of both of them improved compression and tensile strength, whereas the addition of silica fumed itself improved impact strength but supposed a loss in bending and hardness strength. Moreover, the addition of fly ash itself improved hardness strength but the impact strength decreased.

A. H. Majeed [20] added silica fumed particles to an epoxy resin and analyzed its behavior alone and in a CFRC. The results showed an improvement in hardness, compression strength and wave transmission velocity for 2 wt% of silica fumed. Furthermore, A. Christy et al. [21] added SiO_2 NPs into an epoxy resin in percentages until 3 wt% presenting an increase of its tensile and impact properties. S. K. Singh et al. [22] carried out the same study but until higher percentages (up to 8 wt%). Their results showed that, for 4 wt% of SiO_2 NPs, there was an improvement of a 30.57%, 17% and 76% in its tensile strength, flexural strength and flexural modulus respectively. For higher weight percentages, the values started to decrease.

G. Farci et al. [23] studied the impact of the addition of oxyamino triazine (OAT) in the properties of an epoxy. The results showed that there was an improvement of Young modulus, tensile strength, toughness, impact and hardness for a 30 wt% of OAT, whereas A. H. Shah et al. [24] reinforced an epoxy resin with biodegradable Acacia Catechu particles and their analysis showed and improvement of a 52% and 94 % in toughness and hardness respectively for a 1 wt% of particles.

S. Han et al. [25] studied the effect of the addition of graphene nanoplatelets (GNPs) and carbon nanotubes (CNTs) into an epoxy adhesive. They improved the tensile strength in a 20% and 23% for a 0.125 vol% of GNPs and a 0.25 vol% of CNTs respectively. Moreover, the Young's modulus also improved in a 68% and 80% for a 0.5 vol% of GNPs and CNTs respectively.

Apart from the mechanical properties, some researches focus also on the improvement of the thermal properties and some examples of them are next exposed.

The previously remarked work of G. Farci et al. [23] about the addition of OAT in an epoxy also revealed that the thermal resistance of the modified epoxy improved for a 50 wt%. Furthermore, the research of A. H. Shah et al. [24] of the improvement of an epoxy resin by adding biodegradable Acacia Catechu particles showed that the thermal stability was improved and, moreover, the degradation temperature peak was moved from 403 to 442 ºC/min for a 2 wt%.

K. H. Lee et al. [26] studied the thermal effect of using graphite and alumina as fillers of an epoxy resin. The results showed that when the amount of graphite increased, the in-plane thermal conductivity was improved but the out-of-plane thermal conductivity was slightly reduced. Moreover, when both were added, the out-of-plane thermal conductivity was better than the one obtained with the addition of the alumina itself. Moreover, J. Chen et al. [27] studied the effect of purification of CNTs when added into an epoxy resin. The results showed that high purified CNTs improved the thermal conductivity of the resin, however, it was a smaller improvement than the expected one.

M. Zhu et al. [28] analyzed the effect in the thermal conductivity of an epoxy resin of the addition of boron nitride nanocomponents. In order to do that, they added boron nitride nanosheets (BNNS), boron nitride nanoparticles (BNNP) and boron nitride nanotubes (BNNT). The results showed that BNNS have a better effect whereas BNNP have the lowest. For a 3 vol% of BNNS the thermal conductivity improved in a 239%, while D. Matykiewicz et al. [29] analyzed the behaviour of an epoxy resin with basalt powder as filler. They observed that the thermal properties were improved and that the basalt powder provided the resin with a protective effect against fire and elevated temperatures.

In addition, there are some researches about the evolution of electrical and magnetic properties of an epoxy resin when some filler is added.

A. Radón et al. [30] studied the electrical properties of an epoxy composite containing Fe_3O_4 NPs. Their study showed an improvement in the electromagnetic interference (EMI) shielding and the microwave absorption (MA) properties. This modified epoxy also showed high activation and hopping energy. R. Hashjin et al. [31] added graphene nanoplatelets into an epoxy resin and that led to an improvement of the electrical conductivity of 13 orders for a 2.5 wt% of filler. Furthermore, Y. Chen et al. [32] studied the influence of the addition of α-alumina NPs in the electrical insulation of an epoxy resin. The results showed an improvement for de DC volume resistivity at 30ºC from $9.4x10^{17}$ Ωcm to $2.2x10^{18}$ Ωcm.

Chapter 3. Materials and methods

In this chapter the materials that are used are presented. There is also an explanation of the manufacturing process that is being followed in order to obtain the desired materials. Moreover, the tests that are performed to obtain the characterization of the resins are explained.

3.1. Raw materials

Having the objective of manufacture and characterize a modified epoxy resin, there is a need to obtain a set of specimens. With that purpose, the selected epoxy resin is a SR 8100 provided by *Sicomin* that is used along a hardener SD 8824 provided by *Sicomin* too.

After the work about the impact on electrical properties of the addition Fe_3O_4 particles in an epoxy resin carried out by A. Radón [30], a magnetic iron oxide, Fe_3O_4 provided by *Fisher Scientific* in order to study if, apart from the electrical properties, several properties of the epoxy resin are enhanced.

Motivated by the work of A. Christy et al. [21] and S. K. Singh et al. [22] particles of SiO_2 fumed are selected as filler to study, mainly, the evolution of the mechanical properties. In this case silica microparticles provided by *Aldrich Chemistry* is selected.

Table 3.1 sums up the density and particle size values of all the materials applied whereas Table 3.2 summarizes some theoretical properties of the mixture of the epoxy resin and the hardener after a curing cycle of 24 hours at room temperature and 24 hours at 40ºC, provided by the supplier [33].

Table 3. 1. Properties of the used materials

	ρ_{th} (g/cm^3)	D_{50} (μm)
Epoxy resin	1.158	-
Hardener	0.944	-
Fe_3O_4	5.180	1.055
SiO_2 fumed	0.368	0.007

Table 3. 2. Properties of SD1000/SD8824 mixture

Tensile strength (N/mm^2)	60
Tensile modulus (N/mm^2)	2900
Flexural strength (N/mm^2)	108
Flexural modulus (N/mm^2)	3000
T_g (ºC)	63

3.2. Manufacturing process

The samples are obtained in the shape of a square plate of 140x140 mm. With this objective, some molds are prepared with these dimensions made of paperboard, which are placed over a glass plate, as shown in Figure 3.1.

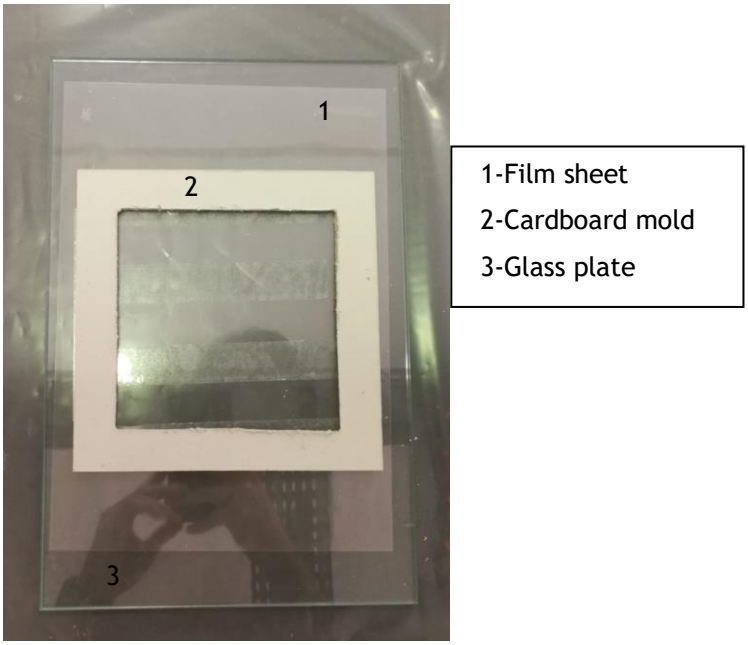

Figure 3. 1. Cardboard mold placed over the glass plate

In order to obtain control samples of the epoxy resin, the hardener is added to the resin in a proportion of 100/22, as indicated by the supplier. It is mixed by a glass rod for 10 minutes and it is poured carefully into the mold until it is completely filled and uniformly distributed. After that, another glass plate is placed over it with a heavy object on top. It is left for 24 hours at room temperature and, after that, 24 hours more at 40ºC inside a *Termolab* oven (Figure 3.2) to complete the curing process.

Figure 3. 2. Oven employed (*Termolab*) for the curing cycle

With the objective of obtaining several samples and a good mixture of Fe_3O_4 particles and the epoxy resin, different percentages (0.25 wt%, 0.5 wt% and 1 wt%) are added into the resin and mixed inside an ultrasonic machine from *GT Sonic* at 1000 rpm for 3 hours with a mixer from *Ibx instruments* (Figure 3.3). In order to control the temperature of the mixture and prevent the overheating, some ice is introduced systematically into the water. Once these 3 hours have past, the resulting mixture is introduced inside a vacuum chamber from *Baco Eng* (Figure 3.4) for three periods of 30 minutes in order to delete possible air bubbles produced due to the velocity of the mixing. After this vacuum process, the procedure is the same that is previously explained: the hardener is added in a 100/22 proportion and mixed for 10 minutes by a glass rod, the mixture is poured into the mold and left 24 hours at room temperature and 24 hours more at 40ºC inside an oven (Figure 3.2) as the curing process.

1-Mixer

2-Ultrasound machine

Figure 3. 3. Ultrasonic machine (*GT Sonic*) and mixer (*Ibx Instruments*) employed

Figure 3. 4. Vacuum chamber employed (*Baco Eng*)

In the case of the SiO_2 fumed particles, the same procedure is followed but changing the quantities of it (2 wt% and 4 wt%). However, due to the high volume of a 4 wt% of SiO_2 fumed particles because of its low density, the resultant mixture has a very high viscosity, making it difficult to mix the hardener and, as a result of that, an non-uniform and plenty of air bubbles sample is obtained. For that reason, this 4 wt% sample is repeated but, without cooling down the mixture while performing the ultrasonic mix in order to increase its temperature and, along with it, reduce it viscosity. As a result of this method, a more uniform sample is obtained and the amount of air bubbles is significantly reduced.

3.2. Experimental setup

3.3.1. Physical tests

The Archimedes' principle states that any body completely or partially submerged in a fluid at rest is acted upon by an upward force of magnitude equal to the weight of the fluid displaced by the body. The specific mass or density (ρ) is obtained following equation 1.

$$\rho = \frac{m}{V} \tag{1}$$

Where:

m is the mass

V is the volume

It is possible to determine the real density and the apparent porosity of the specimens following the standard ASTM C20-00 for apparent porosity, water absorption, apparent specific gravity, and bulk density of burned refractory brick shapes by boiling water [34].

The dry weight (D_w) of the specimens are measured as the standard states, after dried for two hours. These measurements take place in the *Oertling VA204* (Figure 3.5). After that, the specimens are left submersed in water for 24 hours as part of the saturation process. Once this period is over, the saturated weight (W) is measured in the same configuration as for the dry weight. Finally the suspended weight (S) is measured changing the configuration as described in the standard and it can be seen in Figure 3.6.

Figure 3. 5. Measurement equipement (*Oertling VA204*)

Figure 3. 6. Measurement equipement (*Oertling VA204*) configuration to measure Suspended Weight

The first thing that is needed to calculate the density is the exterior volume (V_e). It is obtained, in cm^3, by substracting the suspended weight from the saturated weight, as shown in the equation 2. In this calculus, the density of the water is assumed to be equal to 1.

$$V_e = W - S \tag{2}$$

Once this value is obtained, the density (ρ) is obtained, in g/cm^3, by dividing the dry weight (D_w) by the exterior volume (V_e), as shown in equation 3.

$$\rho = \frac{D_w}{V_e} \tag{3}$$

Furthermore, it is possible to obtain the apparent porosity (P_A), as a percentage by following equation 4.

$$P_A = \frac{W - D_w}{V_e} \cdot 100 \tag{4}$$

3.3.2. Thermal tests

Differential scanning calorimetry (DSC) is a technique that enables to observe fusion, christalization, glass transition temperature (T_g) or even oxidation and other chemical reactions. As the temperature of an amorphous solid increases, glass transitions may occur and it appears as a baseline step of the DSC signal, due to the change in heat capacity of the sample [35].

With the increasing in temperature, the solid becomes less viscous until some point in which the molecules have enough motion freedom to arrange themselves in a chrystaline form. The temparature at which this occurs is called crystallization temperature (T_c). The transition from amorphous to crystaline is an exothermic process and is shown in the DSC signal as a peak. If the temperature continues increasing, eventually it will reach the melting temperature (T_m), resulting and endothermic peak in the DSC signal [34].

In order to analyze the T_g, the glass transition of each sample, with cylindrical shape with 6 mm of diameter and 1 mm of thickness, is analyzed by using DSC (*Netzsch DSC 204* equipment) with a constant heating rate of 10 ºC/min until 150ºC under nitrogen atmosphere. For the epoxy resin, three tests are performed and for each of the composites one test is performed.

The standard ASTM E1356 test method for assignment of the glass transition temperatures by differential scanning calorimetry [36] distinguishes three different

temperatures that are obtained in order to analyze the glass transition. The first one is the onset temperature, which is the point of intersection of the tangent drawn at the point of greatest slope on the transition curve with the extrapolated baseline prior to the transition. The second one is the inflection temperature, that is the point on the thermal curve corresponding to the peak of the first derivative of the parent thermal curve. And finally, the end temperature, which is the point of intersection of the tangent drawn at the point of greatest slope on the transition curve with the extrapolated baseline following the transition.

3.3.3. Mechanical tests

In order to prepare the samples for the performed tests, the plates are cutted in rectangular sections of 10 mm of width, 75 mm of length and 2.2 mm of thickness with a *Struers Accutom-2* that can be seen in Figure 3.7.

Figure 3. 7. Cutting machine empolyed (*Struers Accutom-2*)

Flexural Tests

In order to characterize the flexural stress and strain, three-point bending tests are conducted in the universal testing machine *Shimadzu AGS-X* (Figure 3.8) using the software *Trapezium X Version 1.4.0*. to acquire the tests data. These tests are performed following the ASTM D790-03 standard method for flexural properties of unreinforced and reinforced plastics and electrical insulating materials [37].

Figure 3. 8. Universal testing machine (*Shimadzu AGS-X*)

At least five different specimens of each composition are tested. Their dimensions are measured and Figure 3.9 is a sketch of how these dimensions are called, whereas figure 3.10 shows the configuration of the equipment.

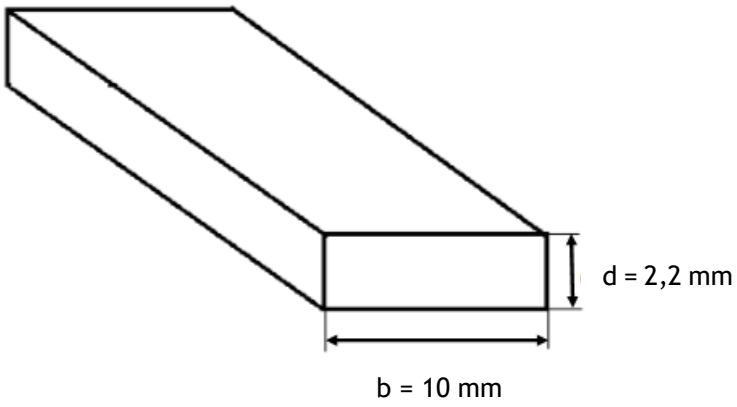

Figure 3. 9. Sketch of the obtained specimens

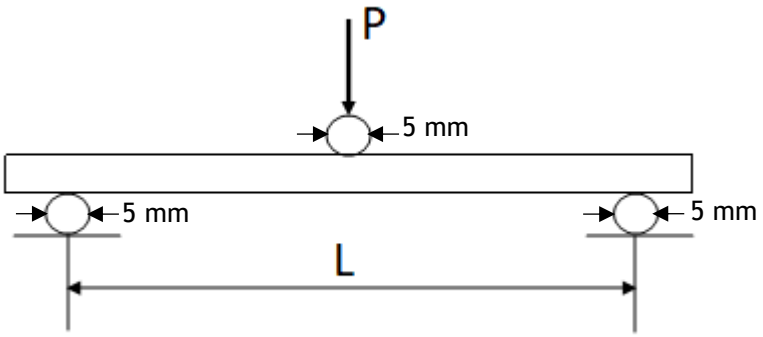

Figure 3. 10. Sketch of the configuration for the mechanical tests

According to the standard ASTM D790 [37], the needed parameters to carry out these tests are the support span (*L*) and the rate of crosshead motion rate (*R*). The standard states that the support span has to be 16 times the thickness of the tested specimen, establishing a span of *L*=40 mm.

In the case of the crosshead motion rate, is obtained following the equation 5 with the result of *R*=1.1 mm/min for the control and Fe_3O_4 specimens and *R*=1.3 mm/min for the SiO_2 fumed specimens.

$$R = \frac{ZL^2}{6d} \tag{5}$$

Where:

Z is the rate of straining of the outer fiber (0.01)
d is the depth of the specimen

The output of these flexural tests are the load of the force applied (*P*) and the deflection at the center of the beam (*D*), along with the elapsed time. In order to analyze the results properly, they are normalized to the respective parameters: flexural stress (σ) and strain (ε). These parameteres are obtained following the equation 6 and 7 respectively.

$$\sigma = \frac{3PL}{2bd^2} \tag{6}$$

$$\varepsilon = \frac{6Dd}{L^2} \tag{7}$$

Where:
b is the width of the specimen

Stress relaxation

In order to analyze the viscoelastic behavior of the polymers, some stress relaxation tests are performed after the obtention of the results of the flexural tests, which show the evolution of the stress along the time. They are performed in three different specimens of the modified resins that showed the highest value of maximum stress for each filler (0.25 wt% Fe_3O_4 and 4 wt% SiO_2), along with specimens from the control resin. These tests take place in the same universal testing machine *Shimadzu AGS-X* and using the same software *Trapezium X Version 1.4.0*. to acquire the tests data. In this kind of test, the maximum load of the force applied is an input. In the case of the performed tests, the value of this input is an 80% of the maximum stress obtained previously. In order to obtain this value for each specimen, *P* is isolated from equation 2. These tests consists of submitting the speciments to a particular load and once it is applied, maintaining the deflection constant for a period of time, in this case 3 hours, by modifying the load applied. The obtained output data are again the load applied (*P*), the deflection at the center of the beam (*D*) and time. In order to analyze the results, the load is normalized again following previous equation 6.

Fracture toughness

Moreover, with the objective of analyze the fracture toughness, some single edge notch bend (SENB) tests are perfromed. In order to do that, and following the ASTM D5045 standard test methods for plane-strain fracture toughness and strain energy release rate of plastic materials [38], beams with the shape represented in Figure 3.11 are obtained cutting the speciemens that were previously obltained.

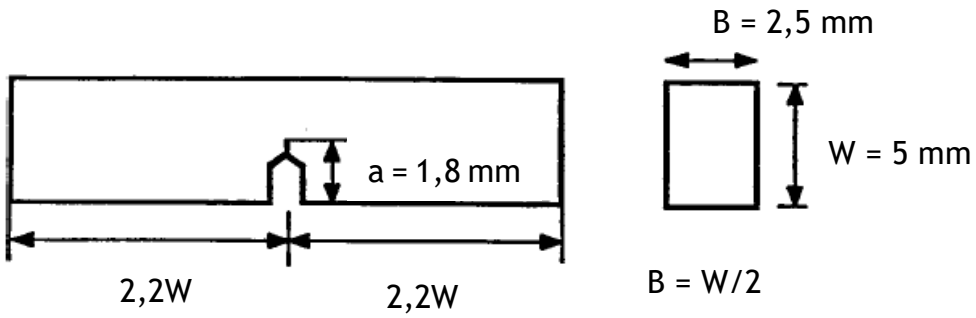

Figure 3. 11. Sketch of the obtained specimens for SENB tests

To carry out the tests, six different speciemens of each composition are tested in the universal testing machine *Shimadzu AGS-X* using the *Trapezium X Version 1.4.0* software. The configuration of the testing machine is represented in Figure 3.12, where the support span is, as specified in the standard, four times the value of W, which is equal to 20 mm. Each test was conducted using a universal testing machine at room temperature under a constant displacement rate of 10 mm/min. The load and displacement at the loading point were measured. The displacement was calibrated based on measured local deformations of the epoxy

specimen at supporting and loading points. Deformation of the stainless steel could be neglected since the stiffness was sufficiently larger than that of the specimen.

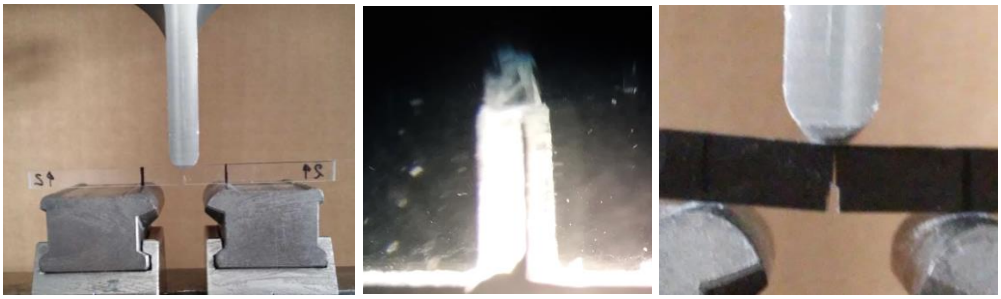

Figure 3. 12. Configuration of the testing machine for SENB tests, pre-crack sharped and open of SENB

The output of these tests are the same as the three point bending tests: the load of the force applied (*P*) and the deflection at the center of the beam (*D*), along with the elapsed time. However, the most important parameter in order to obtain the value of K_{IC} is the load at the break (P_b).

After obtaining the data from the tests, K_{IC} values are obtained following the equations 8 and 9 [38].

$$K_{IC} = \frac{P_b}{BW^{1/2}} f(x) \tag{8}$$

$$f(x) = 6(x)^{1/2} \frac{[1.9 - x(1-x)(2.15 - 3.93x) + 2.72x^2]}{(1+2x)(1-x)^{3/2}} \tag{9}$$

Where:

x is *a*/*W*

Chapter 4. Results and discussion

In this chapter the results obtained from the tests that are explained in the previous chapter are presented and analyzed. After all the data from the tests are obtained and normalized as explained in the previous chapter, the data are treated dividing them in two different parts, one for each filler.

4.1. Physical properties

4.1.1. Density and porosity

Apart from the data obtained following the procedure explained in the previous chapter, other properties of the specimens are obtained. These properties are the theoretical density (ρ_{th}), the relative density (ρ_r) and the total porosity (P_T), following the equations 10, 11 and 12 respectively. However, in order to apply the equation 8, the volume percentages are needed, so they are obtained following equation 13.

$$\rho_{th} = V_m \cdot \rho_m + V_f \cdot \rho_f \tag{10}$$

$$\rho_r = \frac{\rho}{\rho_{th}} \tag{11}$$

$$P_t = 1 - \rho_r \tag{12}$$

$$V_m = \frac{\frac{W_m}{\rho_m}}{\frac{W_m}{\rho_m} + \frac{W_f}{\rho_f}} \tag{13}$$

Where:

V_m is the volume fraction of the matrix
ρ_m is the density of the matrix
V_f is the volume fraction of the reinforcement
ρ_f is the density of the reinforcement
W_m is the weight fraction of the matrix
W_f is the weight fraction of the reinforcement

After all the calculations, the results are summed up in Table 4.1 and Table 4.2, which show the results for the compositions with Fe_3O_4 and SiO_2 respectively.

Table 4. 1. Densities and porosities of the Fe_3O_4 doped specimens

Fe_3O_4 (wt%)	0.25	0.5	1
ρ (g/cm^3)	1.171±0.007	1.185±0.002	1.181±0.002
ρ_{th} (g/cm^3)	1.179	1.182	1.186
ρ_r	0.992	1.002	0.995
P_A (%)	0.506±0.038	0.292±0.044	0.486±0.066
P_T (%)	0.745	0.236	0.446

Table 4. 2. Densities and porosities of the SiO_2 doped specimens

SiO_2 fumed (wt%)	2	4
ρ (g/cm^3)	1.191±0.001	1.195±0.003
ρ_{th} (g/cm^3)	1.128	1.082
ρ_r	1.056	1.104
P_A (%)	0.354±0.052	0.277±0.086
P_T (%)	5.635	10.383

The results of this Archimedes' principle test showed that the specimens obtained from the unfilled epoxy resin and the resin filled with Fe_3O_4 have a real density slightly different from the theoretical one but due to a relatively low porosity (lower than 1%). However, the specimens with SiO_2 show a higher difference between the real density and the theoretical one, due to the high porosity (5.635% and 10.383% for 2 wt% and 4 wt% respectively). This could be due to the high volume that these amounts of SiO_2 meant and the high viscosity of the resultant composition, which difficult the mixture with the hardener, filling the obtained specimens with air bubbles.

4.2. Thermal properties

After the DSC tests are performed, in order to determine the glass transition temperature, the DSC curve for each mixture is represented. Figure 4.1 shows theses curves for the addition of Fe_3O_4 particles.

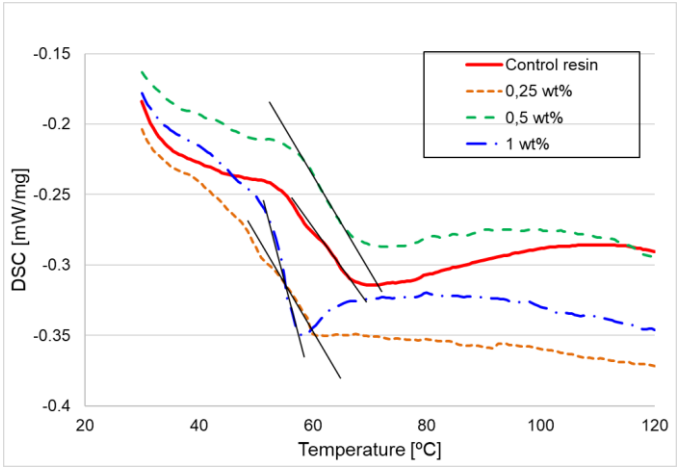

Figure 4. 1. DSC curves of Fe_3O_4 doped specimens

Moreover, the T_g results are presented in Table 4.3, differentiating onset, inflection and end glass transition temperatures.

Table 4. 3. Glass transition temperatures of the Fe_3O_4 doped specimens

Fe_3O_4 (wt%)	0	0.25	0.5	1
Onset T_g (ºC)	63.24	58.38	58.51	53.34
Inflection T_g (ºC)	64.23	59.40	60.43	55.23
End T_g (ºC)	65.98	59.73	67.14	55.67

Furthermore, the results for the addition of SiO_2 fumed particles are summed up the same way, represented in Figure 4.2 and Table 4.4.

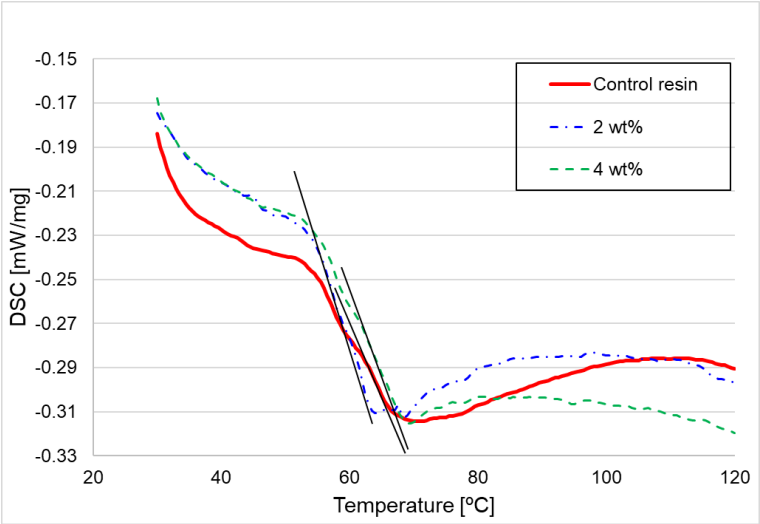

Figure 4. 2. DSC curves of SiO_2 doped specimens

Table 4. 4. Glass transition temperatures of the SiO_2 doped specimens

SiO_2 fumed (wt%)	0	2	4
Onset T_g (ºC)	63.24	61.61	59.11
Inflection T_g (ºC)	64.23	61.97	60.41
End T_g (ºC)	65.98	63.12	61.90

The results for the control resin samples are validated with the information provided by the supplier [33] that states that the DSC onset T_g is 63ºC (see Table 3.2), almost the same value obtained. Moreover, when talking about the results for the addition of the fillers, despite the fact that only a sample of each of them is analyzed, it can be observed that there is a tendency of decrease. It can be due to a poor interfacial interaction between particles and matrix, as stated by J. Jordan et al. [39].

4.3. Mechanical properties

4.3.1. Flexural properties

From these data, the maximum stress (σ_{max}) and the strain at this point (ε_{max}) of each specimen are obtained and an arithmetic mean of them is calculated for each percentage of filler. Moreover, the same is done for the Young's modulus value.

The obtained values of these parameters for the specimens filled with Fe_3O_4 particles are summed up in Table 4.5 while Figure 4.3 and Figure 4.4 show the evolution of σ_{max} and Young's modulus respectively with the addition of these iron oxide particles, in order to be able to make it easier to analyze.

Table 4. 5. Flexural properties of the addition of Fe_3O_4

Fe_3O_4 (wt%)	0	0.25	0.5	1
σ_{max} (MPa)	107.64±3.01	105.91±0.30	105.62±2.30	97.88±4.86
ε_{max} (%)	5.01±0.04	4.68±0.19	5.15±0.12	4.93±0.26
Young's modulus (GPa)	2.81±0.10	2.95±0.17	2.62±0.16	2.50±0.05

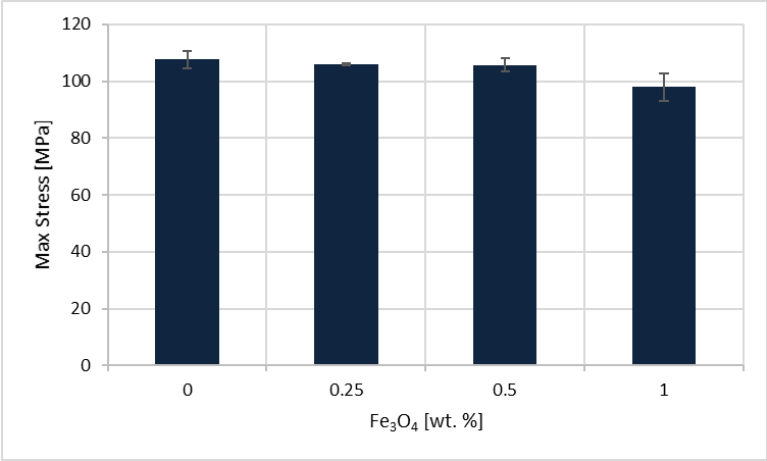

Figure 4. 3. Evolution of max stress with the addition of Fe_3O_4

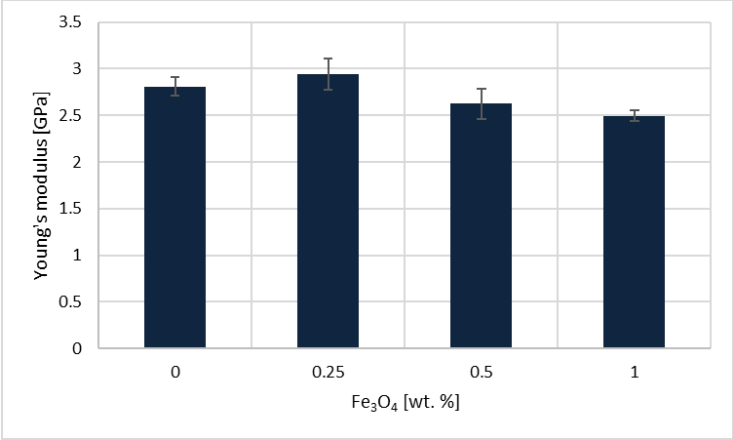

Figure 4. 4. Evolution of Young's modulus with the addition of Fe_3O_4

Furthermore, Figure 4.5 shows the typical stress-strain curves for the different percentages of Fe_3O_4 addition.

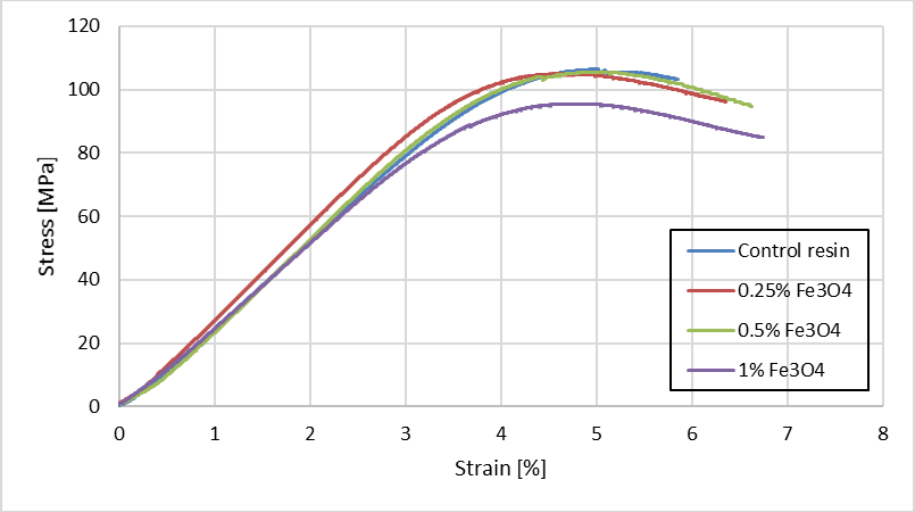

Figure 4. 5. Stress-strain curves of Fe_3O_4 doped specimens

It can be observed that, for a 0.25 wt%, the value of σ_{max} decreases slightly (1.6%) but, on the other hand, the Young's modulus value increases in a 4.84% while the strain at σ_{max} oscillates around 5% for all the amounts of filler.

Furthermore, the addition of SiO_2 fumed particles produced different results for the parameters previously mentioned. In Table 4.6, their values are presented, whereas the evolution of σ_{max} and Young's modulus are represented in Figure 4.6 and Figure 4.7 respectively.

Table 4. 6. Flexural properties of the addition of SiO_2 fumed

SiO_2 fumed (wt%)	0	2	4
σ_{max} (MPa)	107.64±3.01	130.52±3.08	123.91±3.41
ε_{max} (%)	5.01±0.04	4.65±0.26	4.81±0.07
Young's modulus (GPa)	2.81±0.10	3.48±0.49	3.41±0.13

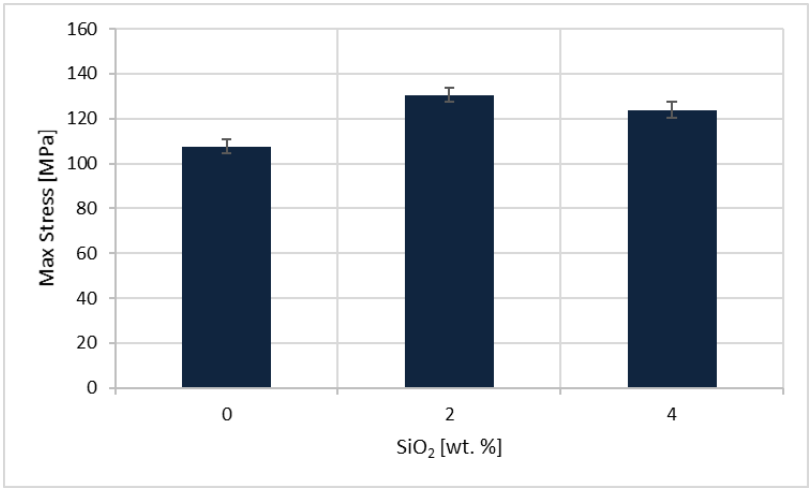

Figure 4. 6. Evolution of max stress with the addition of SiO_2 fumed

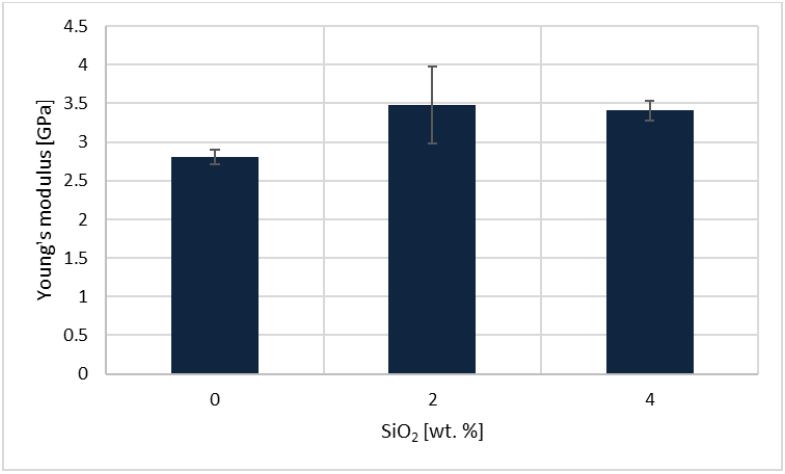

Figure 4. 7. Evolution of Young's modulus with the addition of SiO_2 fumed

Moreover, the Figure 4.8 shows the typical stress-strain curves for the different amounts of SiO_2 fumed particles added to the resin.

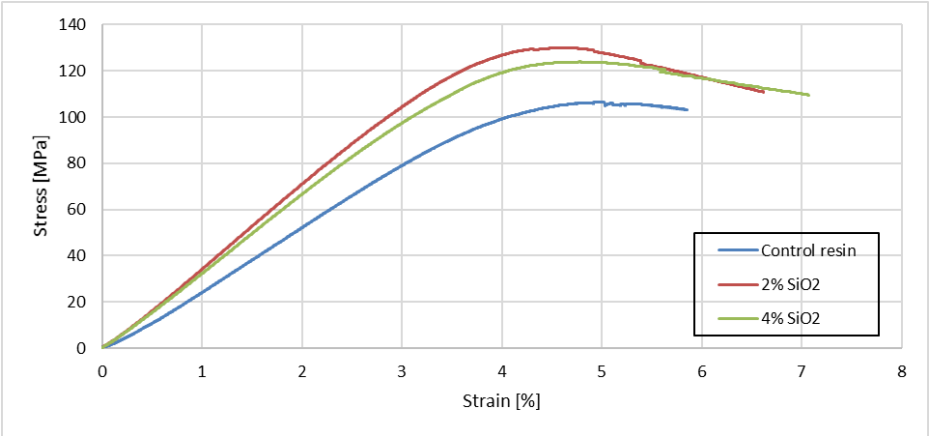

Figure 4. 8. Stress-strain curves of SiO2 doped specimens

The addition of SiO_2 shows an improvement in σ_{max} and Young's modulus of a 21.26% and 23.84% for a 2 wt%. Despite the fact that these improvements are lower for a 4 wt% (15.11% in σ_{max} and 21.36% in Young's modulus), they should be higher but the high porosity of these specimens (see Table 4.2) led to these results being not as good as expexted. In the case of this filler the strain at σ_{max} falls into values below 5%.

Comparing the results of the addition of these two differnet filleres, it can be observed a better flexural performance with the addition of SiO_2 fumed particles due to the fact that it reaches maximum values for a 2 wt% of σ_{max} and Young's modulus, being these values 130.52 MPa and 3.48 GPa respectively, meaning an improvement of 21.26% and 23.84% respectively in comparison with the control resin. On the other hand, in the case of the addition of Fe_3O_4 particles, the only improvement reflected in these results is a 4.84% of improvement in the Young's modulus with the addition of a 0.25 wt% even though it comes with a slight decrease in σ_{max}.

The improvement in σ_{max} with the addition of SiO_2 fumed particles can be compared with the results obtained with the addition of Fe_2O_3 particles carried out by Rajaduari A. et al. [18]. In this case the improvement is only a 9.7%, less than the half of the improvement with the SiO_2 fumed. In the case of the addition of $CaCO_3$ nanoparticles from the work of V. Eskizeybek et al., for a 2 wt% of it the improvement is a 53.4%, much more than the studied case [15]. However, if it is compared with the addition of SiO_2 nanoparticles that is studied by S. K. Singh et al. the improvement is slightly better, being in this case, for a 4 wt% a 17% of improvement [22].

4.3.2. Stress relaxation

After normalizing the data obtained from the software and obtaining the values of σ, and, in order to be able to compare the influence of both fillers in stress relaxation terms, these stress values are converted to non-dimensional values by dividing them by the maximum value of stress. Once these values are obtained, they are plotted in a graph representing the evolution of the stress along the time. This evolution is shown in Figure 4.9.

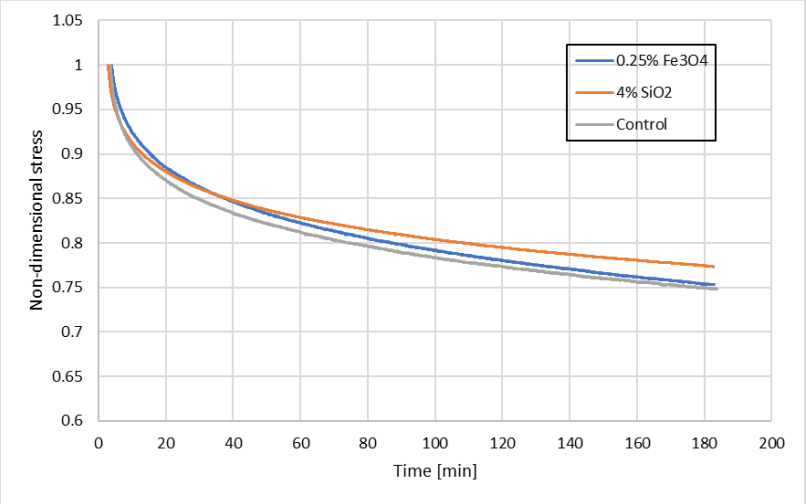

Figure 4. 9. Evolution of the stress relaxation when added the fillers

It can be seen that the control specimens showed a relaxation of a 25.14% while the specimens of 0.25 wt% Fe_3O_4 and 4 wt% SiO_2 showed values of 24.70% and 22.68% respectively. These values mean an improvement in stress relaxation but in a very slightly way.

4.3.3. Fracture toughness

The fracture toughness characterizes the resistance of a material to fracture in a neutral environment in the presence of a sharp crack under severe tensile constraint, such that the state of stress near the crack front approaches plane strain, and the crack-tip plastic (or non-linear viscoelastic) region is small compared with the crack size and specimen dimensions in the constraint direction. The K_{IC} value represent a lower limiting value of fracture toughness and this value is used to estimate the relation between failure stress and defect size for a material in service [38].

The results are obtained for each filler and the results for the addition of Fe_3O_4 particles are summed up in Table 4.7.

Table 4. 7. Fracture toughness of Fe_3O_4 doped specimens

Fe_3O_4 (wt%)	0	0.25	0.5	1
K_{IC} (MPa·m$^{1/2}$)	2.13±0.05	2.15±0.13	2.12±0.1	2.01±0.07

In order to make it easier to analyze, these results are presented in a plot in Figure 4.10.

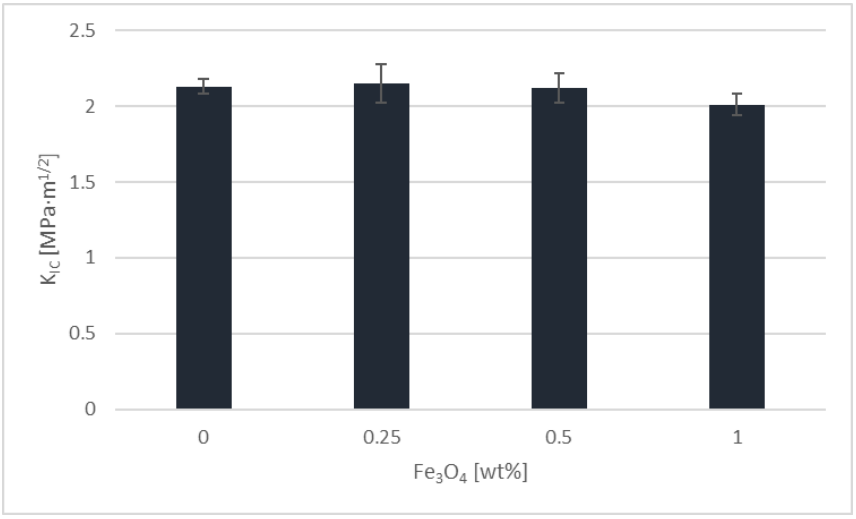

Figure 4. 10. Evolution of K_{IC} with the addition of Fe_3O_4

As it can be observed, there is a very slight improvement for the addition of a 0.25 wt% in only a 0.94%.

Moreover, the results for the SiO_2 fumed particles are shown in Table 4.8.

Table 4. 8. Fracture toughness of SiO_2 doped specimens

SiO_2 (wt%)	0	2	4
K_{IC} (MPa·m$^{1/2}$)	2.13±0.05	2.32±0.19	2.05±0.17

As it is done before, these results are also shown in the shape of a plot in Figure 4.11.

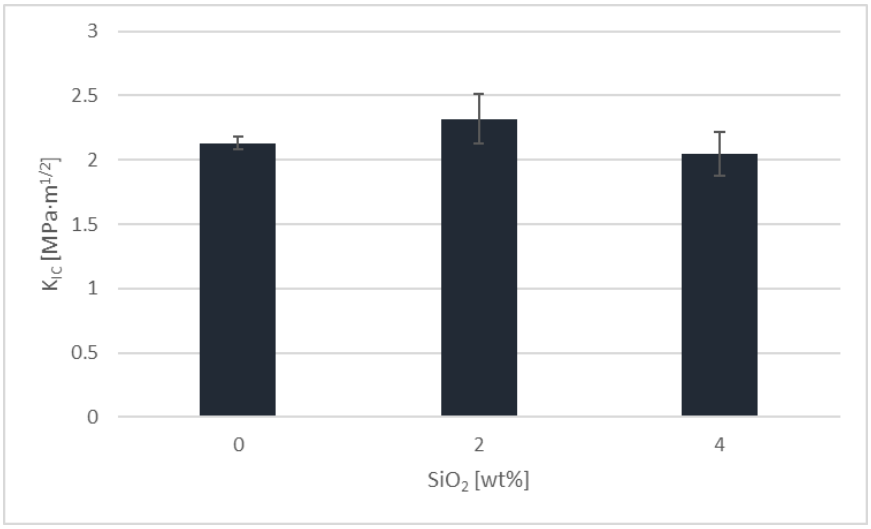

Figure 4. 11. Evolution of K_{IC} with the addition of SiO_2 fumed

In this case, for the addition of a 2 wt% of SiO_2 fumed particles, there is an increase of a 8.92%.

As it happened for the previously studied mechanical properties, K_{IC} improves in a higher way with the addition of SiO_2 fumed than with the addition of Fe_3O_4. Moreover, this improvement is way smaller compared with the increasings reached with the addition of Fe_2O_3 NPs by T. Sun et al. [17] that achieved an improvement in K_{IC} of a 106% for a 4 wt% or with the addition of TiO_2 micro and nanoparticles by S. K. Singh et al. [16] that achieved a 44.95% and 141.85% of improvement for a 4 wt% of microparticles and a 6 wt% of nanoparticles respectively.

A possible limitation of the experimental result can be related with the poor distribution of the fillers in the epoxy matrix. In order to identify this problem several microscopic images are performed. Thus, EDX mapping is applied in order to analyze the distribution of the particles of Fe_3O_4 and SiO_2 in the epoxy matrix.

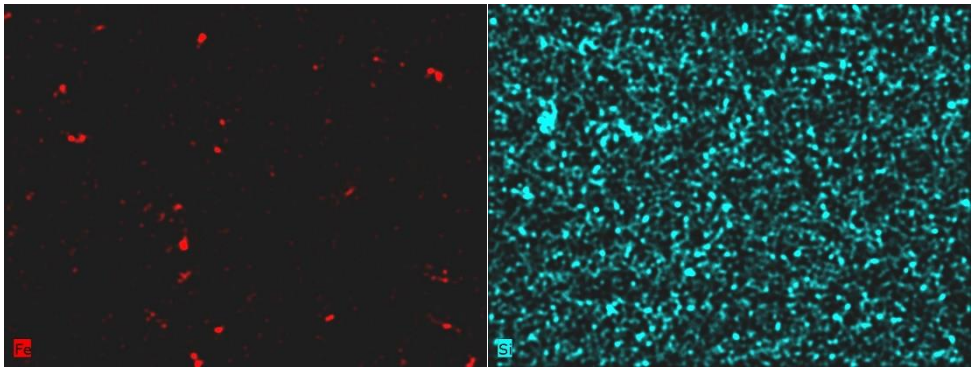

a) b)

Figure 4. 12. Mapping distribution of fillers in epoxy resin: a) Filler of 1 wt% Fe_3O_4 b) Filler of 4 wt% SiO_2

From these images it can be observed that the fillers are distributed in a homogeneous form and no relevant cluster are present. However, in these images is not possible visualize, in a correct way, the air bubbles. Also the interface quality between the particles and the epoxy matrix is not detailed observed.

Chapter 5. Final conclusions and future work

5.1.Conclusions

In this work the methodology of manufacture composites of epoxy resin with fillers of SiO_2 and Fe_3O_4 is developed. Several samples of epoxy/SiO_2 and epoxy/Fe_3O_4 is characterized in physical, mechanical and thermal properties. The results obtained are discussed with the literature .

After analyzing the obtained results, in order to sum up, some conclusions can be taken into considaration:

- The addition of SiO_2 fumed particles presented an obstacle due to its low density, which leads into a high porosity due to the high viscosity of the mixture.
- Glass transition temperature (T_g) presents a decrease with the addition of both fillers.
- With the addition of Fe_3O_4 particles, the maximum stress (σ_{max}) decreases. However, for a 0.25 wt% there is a slight improvement in the Young's modulus of a 4.84%.
- With the addition of SiO_2 fumed particles, there is an improvement in σ_{max} and Young's modulus being the highest improvement for a 2 wt% (21.26% and 23.84% respectively).
- The stress relaxation of the resin suffers a slight improvement when adding Fe_3O_4 or SiO_2 fumed particles in a 0.25 wt% and 4 wt% respectively. However, this improvement is no significant enough in order to apply it into a component (0.36% and 2.46% for Fe_3O_4 and SiO_2 fumed respectively).
- With the addition of Fe_3O_4 particles, the value of K_{IC} presents a slight increase (0.94%) for a 0.25 wt%.
- With the addition of SiO_2 fumed particles, there is an increase in K_{IC}, achieving an increase of 8.92% for a 2 wt%.

5.2. Future work

After studying the obtained results, some future work could be projected. For instance, the epoxy resin filled with Fe_3O_4 shows a magnetical behavior when a strong magnet is approached, so it could be interesting to study and analyze its electromagnetic properties.

Moreover, a study of the internal surface of the 4 wt% SiO_2 specimens could be analyzed in order to apply a correction to the obtained values of their mechanical properties. Furthermore, after observing the issues that the addition of SiO_2 particles means, a more accurate procedure to reduce the viscosity of the mixture could be applied in order to be able to obtain better results and study the evolution for amounts above 4 wt%.

After finding that there was a bad quality of the interface, a surface treatment could be applied, as the one based on a silane treatment used by J. O. Park et al. [40], that improved interfacial adhesive strength, along with the magnetic properties of a Fe_3O_4/epoxy nanocomposite.

Moreover, both fillers could be added at the same time as did by D. Luo et al. [41], who achieved an optimization of the magnetic performance after adding both Fe_3O_4 and SiO_2 nanoparticles.

Furthermore, other properties could be analyzed, such as tensile properties, impact resistance properties, hardness or even thermal and electrical conductivity.

References

[1] W. Callister and D. Retwisch, "Materials science and engineering: an introduction," 7th ed., vol.97. United States, 2007.

[2] M. F. Ashby, "Materials and Sustainable Development," Butterwoth-Heinemann, 2016.

[3] A. P. Mouritz, "2-Aerospace materials: past, present and future A2 - Introduction to Aerospace Materials," Woodhead Publishing, 2012.

[4] A. P. Mouritz, "15-Fibre-polymer composites for aerospace structures and engines - Introduction to Aerospace Materials," Woodhead Publishing, 2012.

[5] A. P. Mouritz, "13-Polymers for aerospace structures - Introduction to Aerospace Materials," Woodhead Publishing, 2012.

[6] I. Hamerton and J. Kratz, "Thermosets," 2nd ed., Bristol, United Kingdom, 2018.

[7] M. D. Banea and L. F. M. da Silva, "Adhesively bonded joints in composite materials: An overview," Proc. Inst. Mech. Eng. Part L J. Mater. Des. Appl., no. 1, 2009.

[8] J. A. Bishopp, "The history of Redux and the Redux bonding process," Int. J. Adhes., vol. 4, no. 17, 1997.

[9] D. M. Brewis, "Handbook of adhesive technology," vol.15, no. 4, 1995.

[10] A. Baldan, "Adhesively-bonded joints and repairs in metallic alloys, polymers and composite materials: Adhesives, adhesion theories and surface pretreatment," *Journal of Materials Science*, vol. 39, no. 1, 2004.

[11] M. Dekker, "Composites Engineering Handbook," 11th ed., New York, United States, 1997.

[12] S. M. Sapuan, "Composite Materials," Concurrent Engineering Approach, 2017.

[13] ASTM Standard D5573-99, "Standard practice for classifying failure modes in fibre-reinforced-plastic (FRP) joints," ASTM International, West Conshohocken, PA, 1999.

[14] D. Bazrgari el al., "Mechanical properties and tribiological performance of epoxy/Al_2O_3 nanocomposite," Ceramics International, vol. 44, 2018.

[15] V. Eskizeybek et al., "Static and dynamic mechanical responses of $CaCO_3$ nanoparticle

modified epoxy/carbon fiber composite," Composites Part B: Engineering, vol. 140, 2018.

[16] S. K. Singh et al., "Thermo-mechanical behaviour of TiO_2 dispersed epoxy composites," Engineering Fracture Mechanics, vol. 184, 2017.

[17] T. Sun et al., "Modified nano Fe_2O_3-epoxy composite with enhanced mechanical properties," Materials & Design, vol. 87, 2015.

[18] V. R. Arun Prakash and A. Rajadurai, "Thermo-mechanical characterization of siliconized E-glass fiber/hematite particles reinforced epoxy resin hybrid composite," Applied Surface Science, vol. 384, 2016.

[19] N. Saleh and M. H. Al-Maamori, "Evaluating the mechanical properties of Epoxy resin with Fly ash and Silica fume as fillers," Advances in Physics Theories and Applications, 2014.

[20] A. H. Majeed, "Enforcement of Epoxy with Silica Fume and Carbon Fiber," Tikrit Journal of Engineering Sciences, 2018.

[21] A. Christy et al., "Development and Analysis of Epoxy/nano SiO_2 Polymer Matrix Composite fabricated by Ultrasonic Vibration assisted Processing," Materials Today: Proceedings 4, 2017.

[22] S. K. Singh et al., "Improving tensile and flexural properties of SiO_2-epoxy polymer nanocomposite," Materials Today: Proceedings 5, 2018.

[23] G. Farzi et al., "Mechanical, thermal and microstructural properties of epoxy-OAT composites," Construction and Building Materials, vol. 197, 2019.

[24] A. H. Shah et al., "Evaluation of mechanical and thermal properties of modified epoxy resin by using acacia catechu particles," Materials Chemistry and Physics, vol. 225, 2019.

[25] S. Han et al., "Mechanical and Electrical Properties of Graphene and Carbon Nanotube Reinforced Epoxy Adhesives: Experimental and Numerical Analysis," Composites: Part A, 2019.

[26] K. H. Lee et al., "Thermal characteristics of epoxy composites with graphite and alumina," Thermochimica Acta, vol. 676, 2019.

[27] J. Chen et al., "Thermal and electrical properties of the epoxy nanocomposites reinforced with purified carbon nanotubes," Materials Letters, 2019.

[28] M. Zhu et al., "Improving thermal conductivity of epoxy resin by filling boron nitride nanomaterials: A molecular dynamics investigation," Computational Materials Science, vol. 164, 2019.

[29] D. Matykiewicz et al., "Basalt powder as an eco-friendly filler for epoxy composites: Thermal and thermo-mechanical properties assessment," Composites Part B, 2018.

[30] A. Radón et al., "Electrical properties of epoxy nanocomposites containing Fe_3O_4 nanoparticles and Fe_3O_4 nanoparticles deposited on the surface of electrochemically exfoliated and oxidized graphite," Applied Surface Science, vol. 474, 2019.

[31] R. Hashjin et al., "Modeling of electrical conductive graphene filled epoxy coatings," Progress in Organic Coatings, vol. 125, 2018.

[32] Y. Chen et al., "Epoxy/α-alumina nanocomposite with high electrical insulation performance," Progress in Natural Science Materials International, vol. 27, 2017.

[33] Sicomin Epoxy Systems, "SR 8100/SD 882X Infusion System" E1436 Data Sheet, 2019.

[34] ASTM Standard C20-00, "Standard test methods for apparent porosity, water absorptions, apparent specific gravity, and bulk density of burned refractory brick and shapes by boiling water," ASTM International, West Conshohocken, PA, 2005.

[35] Dean JA, "The Analytical Chemistry Handbook," McGraw Hill Inc, New York, United States, 1995.

[36] ASTM Standard E1356-08, "Standard test methods for assignment of the glass transition temperatures by differential scanning calorimetry," ASTM International, West Conshohocken, PA, 2008.

[37] ASTM Standard D790-03, "Standard test methods for flexural properties of unreinforced and reinforced plastics and electrical insulating materials," ASTM International, West Conshohocken, PA, 2003.

[38] ASTM Standard D5045-99, "Standard test methods for plane-strain fracture toughness and strain energy release rate of plastic materials," ASTM International, West Conshohocken, PA, 1999.

[39] J. Jordan et al., "Experimental trends in polymer nanocomposites - a review," Materials Science and Engineering, vol. 393, 2005.

[40] J. O. Park et al., "Silane treatment of Fe_3O_4 and its effect on the magnetic and wear properties of Fe_3O_4/epoxy nanocomposites," Applied Surface Science, vol. 256, 2010.

[41] D. Luo et al., "Incorporation of the Fe_3O_4 and SiO_2 nanoparticles in epoxy-modified silicone resin as the coating for soft magnetic composites with enhanced performance," Journal of Magnetism and Magnetic Materials, vol. 452, 2018.